Available online at www.sciencedirect.com
ScienceDirect
Journal of Non-Crystalline Solids 354 (2008) 521–528
JOURNAL OF NON-CRYSTALLINE SOLIDS
www.elsevier.com/locate/jnoncrysol

Structure, chemical durability and crystallization behavior of incinerator-based glassy systems

L. Barbieri [a,*], A. Karamanov [b,c], A. Corradi [a], I. Lancellotti [a], M. Pelino [b], J. Ma. Rincon [d]

[a] Dip. di Ingegneria dei Materiali e dell'Ambiente-University of Modena and Reggio Emilia, Via Vignolese 905, 41100 Modena, Italy
[b] Dip. di Ingegneria Chimica e dei Materiali, University of L'Aquila, 67100 Monteluco di Roio, Italy
[c] Institute of Physical Chemistry, Bulgarian Academy of Sciences, G. Bonchev street, Block 11, 1113 Sofia, Bulgaria
[d] Inst. Torroja de Ciencias de la Construccion CSIC, Serrano Galvache s/n, 28033 Madrid, Spain

Available online 5 November 2007

Abstract

Vitrification by melting is being proposed as a convenient method to solidify different kinds of silicate and other oxide-based inorganic wastes. Incinerator bottom and fly ashes have been mixed with glass cullet, feldspar and clay by-products as melting fluxing agents. Washing, drying, and grinding pre-treatments followed by melting at 1450 °C lead to the formation of glasses and glass-ceramics, depending on the starting materials composition and thermal treatment. The obtained glasses have been studied by SEM, chemical durability tests in aqueous and alkaline environment, leaching test (UNI 10802), and by differential thermal analysis. The glass-ceramics morphology was investigated by XRD and SEM. The results were explained by the structure of the glasses caused by the presence of different amount of modifiers in the glassy lattice. The obtained glasses show good chemical resistance, in particular in alkaline environment and thermal characterization highlighted that the materials are also suitable to obtain glass-ceramics.

PACS: 61.43.Fs; 65.60.+a; 64.70.Pf; 64.70.Dv

Keywords: Chemical durability; Crystallization; Glass-ceramics; Glasses; Silicates; X-ray diffraction

1. Introduction

Vitrification by melting is being proposed as a convenient method to solidify different kinds of silicate and other oxide-based inorganic wastes. The promotion of controlled crystallization by forming partly crystallized materials, such as glass-ceramics, can be a technological solution to convert a waste material into a valuable product. Moreover, vitrification causes the reduction of the waste volume, the increase of the homogeneity of the waste chemical composition and its subsequent conversion into inert materials with interesting chemical and mechanical properties. Depending on the waste composition, glass forming additives are often added to starting raw materials. In this work, incinerator bottom and fly ashes have been mixed with glass cullet or a feldspar and clays by-products as melting fluxing agents. By considering incinerator waste as secondary raw material, it is necessary to distinguish between fly and bottom ashes, which have quite different chemical compositions. Fly ash is particularly problematic because it contains significant concentrations of heavy metals (e.g., As, Pb, Sb, Sn). With regards to bottom ash, the proportions of different constituents are fairly constant [1,2] independent of the waste origin and the particular incineration process. Consequently, bottom ash appears to be a suitable secondary raw material for re-use, for example, in constructions and civil works, due to capabilities of this sector to absorb a high volume of materials. Bottom ash contains typical glass formers and modifiers, such as Si, Al, Ca, and Na, thus it is suitable for vitrification. The most significant advantages of vitrification include volume reduction of the waste, good chemical durability of the final product, and the possibility to use

* Corresponding author. Tel.: +39 059 2056231; fax: +39 059 2056243.
E-mail address: luisa.barbieri@unimore.it (L. Barbieri).

0022-3093/$ - see front matter © 2007 Elsevier B.V. All rights reserved.
doi:10.1016/j.jnoncrysol.2007.07.080

wastes of different origins to obtain more homogeneous batches. The resulting inert vitreous product can be utilized in principle, in various ways: as road-base material; in embankments; as blasting grit; to partially replace sand in concrete; in the production of construction and decorative materials, such as water-permeable blocks, tiles, pavement bricks, and decorative stones for gardens [3–5].

The main part of the literature works is based on vitrification of bottom ash (used as it is or mixed with other waste and/or raw materials) [6,7].

In the present work, glassy compositions containing both incinerator bottom and fly ashes have been prepared. SEM analysis and durability tests have been performed in order to evaluate the glass network stability, while thermal analysis and X-ray diffractometry have been used in order to study the crystallization tendency of the obtained material.

2. Experimental procedures

Incinerator bottom and fly ashes have been mixed with glass cullet (main oxides SiO_2, Al_2O_3, MgO, CaO, and Na_2O), feldspar, and clays by-products (main oxides SiO_2, Al_2O_3, and Na_2O) as melting coadjuvants. The choice of these three additives is due to their different chemical composition. Glass cullet contains high amount of calcium oxides (around 10%), which can favor crystal growth in the glass; feldspar and clay wastes from ceramic industry are particularly rich in alumina (around 20% and 25%, respectively), which renders the glass network more resistant to chemical reagents.

The fly ash characterization required pre-treatments such as water washing to separate and quantify the soluble fraction, which amounts to 14.5 wt% and it is composed mainly by chlorines, K_2O, Na_2O, CaO, SO_4^{2-}, and NO_3^-. Furthermore, the insoluble fraction, corresponding to 85.5%, was analyzed by X-ray-fluorescence (Philips PW 2004). The obtained results are reported in Table 1.

Bottom ash required also some pre-treatments, such as grinding at particle size <0.4 mm and magnetic separation. The chemical analysis has been performed by X-ray-fluorescence (Table 1).

Three batches were prepared by mixing the different raw materials:

(a) V1: 50 wt% bottom ash–5 wt% fly ash–45 wt% glass cullet;
(b) V2: 53 wt% bottom ash–4 wt% fly ash–43 wt% feldspar;
(c) V3: 30 wt% bottom ash–20 wt% clay–50 wt% glass cullet

and the corresponding oxide compositions of the resulting glass are reported in Table 1. The batches were melted at 1450 °C, and the melts were rapidly quenched in air.

The bulk of V1 and V2 glasses, which contain higher amount of bottom and fly ashes than V3, has been observed by scanning electron microscopy (SEM Philips XL 30 coupled with energy dispersion spectroscopy EDAX 9900) to study the glass homogeneity and by X-ray diffraction (Philips PW 3710 with Ni-filtered CuKα radiation) to confirm the amorphous structure of the material. Chemical durability tests (ISO 719 and ISO 695) have also been conducted in order to evaluate the chemical resistance of the prepared glasses in aqueous and alkaline environments, respectively. The eluates were analyzed by pH (pH 6 Euthech Instrument) and conductivity (CON 6 Euthech Instrument) measurements and by inductively coupled plasma (ICP Varian Liberty 200), to investigate the amount and kind of leachate elements.

Table 1
Chemical composition (wt%) of the incinerator ashes and the prepared glasses

Oxide	Fly ash	Bottom ash	V1	V2	V3
SiO_2	18.5	46.7	54.39	52.64	52.57
TiO_2	1.56	0.77	0.58	0.61	0.82
Al_2O_3	7.37	6.86	5.41	12.13	9.07
Fe_2O_3	2.26	4.69	3.84	4.36	3.28
MgO	2.74	2.22	2.47	1.77	1.73
CaO	37.5	26.3	20.31	17.28	16.71
Na_2O	2.93	4.62	8.17	5.88	8.78
K_2O	2.03	0.888	1.12	1.06	1.62
ZnO	2.07	0.714	0.41	0.52	0.21
SO_3	14.4	2.18	0.46	0.35	–
PbO	0.040	0.071	0.051	0.030	0.025
BaO	0.139	0.109	0.159	0.134	0.105
As_2O_3	nd	0.001	0.009	0.008	0.008
Cr_2O_3	0.091	0.074	0.096	0.047	0.055
CuO	0.091	0.281	0.198	0.098	0.175
NiO	0.013	0.011	0.006	0.004	0.005
LOI	8.4	11.0	–	–	–

Glasses have been subjected to 24 h leaching test according to UNI 10802. Samples were placed in bidistilled water with a leaching volume/material weight ratio of 10 l/kg and maintained for 24 h at room temperature. After filtration, the chemical composition of the eluate has been analyzed by ICP (OES Thermo Optek).

The crystallization of the glasses has been studied by DTA (Linseiz L81). The growth mechanism (surface or bulk) was estimated, comparing the traces of fine (<63 μm) and coarse (216–300 μm) glass fractions at 10 °C/min. The activation energy of viscous flow in the glass transition ranges, the crystallization activation energy, and the reaction order were determined by using results obtained at different heating rates (5, 7.5, 10, and 20 °C/min). The preliminary glass-ceramics samples, obtained by means of different heat treatments have been characterized by XRD and SEM techniques.

3. Results

3.1. Structure and chemical durability

The obtained glasses are quite different at an optical observation: V1 appears dark and homogeneous while V2

shows a black bulk with red streaking due to the dispersion of visible light and transmission of infrared, a phenomenon typical for opal and/or phase separated glasses [8,9]. V3, which contains lower amount of municipal solid waste, is characterized by good transparency and dark-green color.

The glasses with high waste amount (i.e. V1 and V2) were analyzed by SEM to verify the presence of micro-heterogeneous zones. SEM analysis of V1 (Fig. 1(a)) points out the presence of a liquid–liquid immiscibility with a non-spinodal structure (i.e. grown by a nucleated-type mechanism). The second phase is separated in isolated spherical drops with an interface having the same degree of sharpness. The droplets having 0.5–2 μm diameter are uniformly and randomly dispersed throughout the matrix, suggesting that liquid–liquid separation may occur during the cooling of the melt. The separated phase does not possess crystalline order and does not affect the amorphous character of the material. In fact, the glassy nature of the whole samples was confirmed by X-ray diffraction, which shows only the broad band of glass with no crystalline phases. In V2 glass (Fig. 1(b)) larger immiscibility zones (3–4 μm) are present. In both glasses, some white dots enriched in copper and sulfur as confirmed by EDS are also evident throughout the samples (particles marked with a circle). According to the chemical analysis of the starting materials these elements derive from both the bottom and fly ashes (Table 1). Similar phase (i.e. Zn–S, Fe–P–S) was observed in other glassy materials produced starting from industrial wastes [9–11].

The chemical durability characterization of V1 and V2 glasses was conducted in order to evaluate the chemical resistance in aqueous and alkaline environments, respectively. This property is strictly related to the different structure of the glasses induced by the presence of different amounts of modifiers in the glassy lattice. The durability tests allow dividing glasses into different categories, where a lower category number corresponds to a better resistance [12]. As far as durability in water is concerned (Table 2(a) and (b)), V1 glass shows medium–high resistance, belonging to class 3, which corresponds to a range of alkali leached between 62 and 264 μg/g, while V2 shows very high resistance, belonging to class 1, which corresponds to a value of alkali element leached <31 μg/g. This behavior is also confirmed by the pH and conductivity measurements. The different degree of dissolution of the two glasses is also demonstrated by the analysis of the amount of network

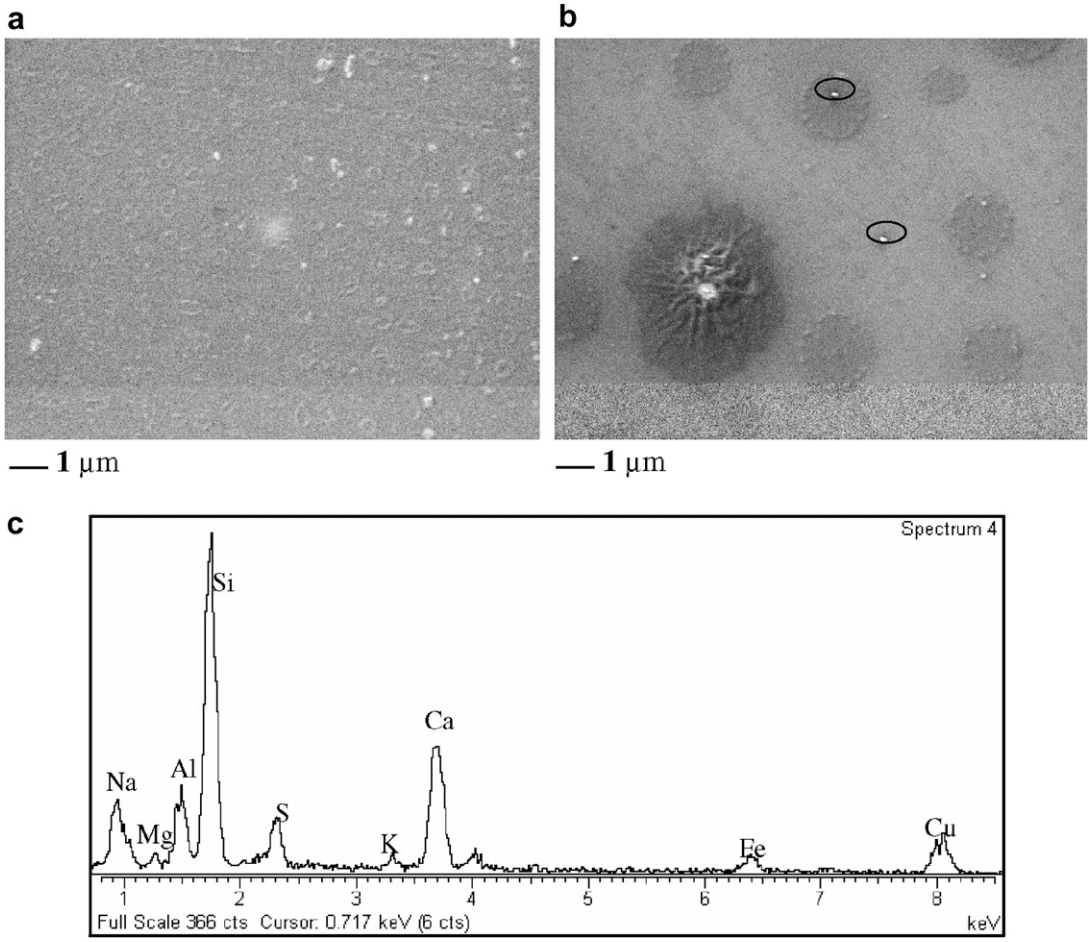

Fig. 1. SEM micrographs of V1 parent glass at 9000× (a) and V2 parent glass at 5000× (b). EDS spectrum of white dots (c).

Table 2
Results of durability tests, pH, and conductivity measurements in aqueous (a) and alkaline (c) environment and ICP analysis of the aqueous environment eluates (b)

Sample	Alkali leached (μg/g)	pH	Conductivity (μS)
(a)			
V1	98.23	8.35	52.2
V2	13.2	7.90	23.3
Distilled water	–	5.48	2.65

	Weight loss (mg/100 m^2)	pH	Conductivity (μS)
(c)			
V1	32.33	12.68	195.4
V2	18.23	12.65	190.1
Alkaline solution	–	12.71	164.7

	Si (ppm)	Al (ppm)	Na (ppm)	K (ppm)
(b)				
V1	2.56	0.09	3.78	0.15
V2	0.08	0.05	0.45	0.07

formers, especially silicon, and modifiers, especially sodium, found in the eluates, which confirm the lower degree of stabilization of the V1 glass lattice (Table 2(b)).

In alkaline environment, however, (Table 2(c)) both glasses are classified by the norm as belonging to class 1, low alkaline attack, which corresponds to a loss in weight <75 mg/100 m^2, even if V1 presents a loss higher with respect to V2. Both glasses show higher values of conductivity with respect to the extraction solution because of the higher amount of mobile ions, while pH values are constant, the environment being already alkaline and therefore less sensible to the variation.

The effectiveness, on immobilizing the heavy metal ions, of incinerator residues vitrification process was confirmed by the 24 h leaching test. Table 3 shows that all the detected elements resulted below the Italian law limits.

3.2. Crystallization behavior

Due to the high tendency toward crystallization, the viscosity vs. temperature curves of the studied glasses could not be experimentally obtained. For this reason the VFT (Vogel–Fulcher–Tammann) equations were estimated by the Lakatos method [13]. Fig. 2 shows the obtained calculated viscosity vs. temperature curves. The average values

Table 3
Glasses leaching test

Element	V1 eluate (mg/l)	V2 eluate (mg/l)	Law limit D.Lgs 13.3.2003
As	<0.05	<0.05	0.05
Ba	<0.02	<0.02	2
Pb	<0.02	<0.02	0.05
Cr	<0.02	<0.02	0.05
Cu	<0.02	<0.02	0.2
Ni	<0.02	<0.02	0.04
Zn	<0.02	<0.02	0.4

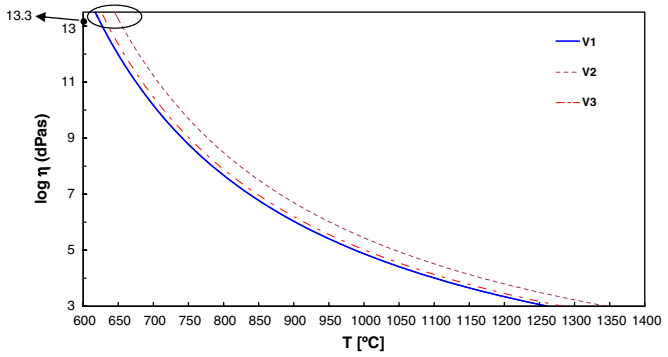

Fig. 2. Hypothetical viscosity–temperature curves of the studied compositions.

of the activation energies of viscous flow, E_η, for different temperature ranges were evaluated applying the Arrhenius equation (Table 4):

$$\eta(T) = \eta_0 \exp(E_\eta/RT). \quad (1)$$

DTA results for the fine (labeled P) and the coarse (labeled B) glass fractions are plotted in Fig. 3. It highlights similar glass transition, T_g, and liquidus, T_l, temperatures for the P and B samples and different crystallization peak temperatures, T_P. The figure shows also that the T_g values obtained by the DTA curves are comparable with the ones calculated by the Lakatos curves (i.e. the temperatures, corresponding to the viscosity value of $10^{13.3}$ dPa s (Fig. 2)). V1-P and V1-B traces show similar sharp crystallization peaks at low temperatures with a T_P shift of only 40 °C, indicating that bulk phase formation occurs in this glass [9,14]. V2 glass shows a less pronounced crystallization trend. V2-P crystallization exotherm peak is characterized by low-intensity and T_P is close to T_l, while no exo-effect occurs in V2-B. V3 composition is characterized by an intermediate behavior: T_P of V3-P sample is at lower temperature than V2-P and low-intensity exo-peak is observed in V3-B. The T_P shift of about 100 °C suggests that surface crystallization is mainly occurring. The different crystallization tendency of studied glasses was confirmed also by the values of the Hruby coefficient, $K_H = (T_P - T_g)/(T_l - T_P)$ [15,16]. This parameter is widely used to evaluate the crystallization ability of the glasses: the higher its value, the lower the crystallization tendency. K_H, obtained by the DTA powder curves, presents values of 1.2, 3.6, and 2.1 for V1, V2, and V3, respectively, confirming the high

Table 4
Variation of the activation energy of viscous flow (kJ/mol) vs. temperature

	600–700 °C	700–800 °C	800–900 °C	900–1000 °C	1000–1100 °C
V1	680	500	400	330	290
V2	780	550	430	360	310
V3	720	520	400	340	300

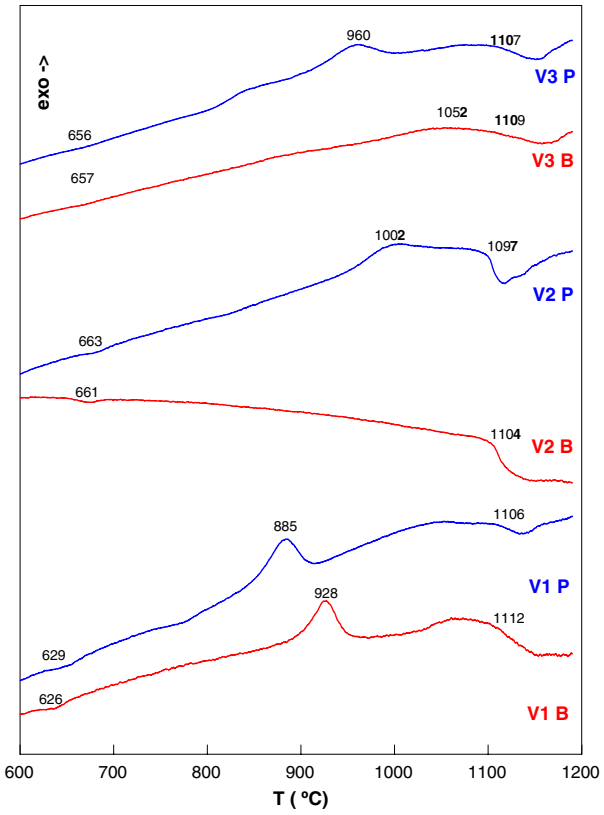

Fig. 3. DTA traces of powder and bulk samples at 10 °C/min.

crystallization ability of V1, intermediate of V3, and scarce of V2.

In order to obtain additional information on the crystallization behavior of V1 and V3, powder samples were studied at different heating rates. The activation energy of viscous flow in glass transition range, E_{T_g}, and the activation energy of crystallization, E_{cr}, were evaluated by the Chen's equation [17]

$$\frac{E_X}{RT_\alpha} = \ln\left(\frac{T_\alpha^2}{v}\right), \tag{2}$$

where T_α are temperatures at which the degree of transformation, α, attains equal value at different heating rates, v. E_{T_g} and E_{cr} were evaluated by the T_g and T_P variations, respectively.

The reaction order (named also Avrami parameter), n, was evaluated by the relationship proposed by Ozawa [18]:

$$\left.\frac{d\{\ln[-\ln(1-\alpha)]\}}{d(\ln v)}\right|_T = -n, \tag{3}$$

where α is evaluated from a number of exothermic peaks, obtained at different heating rates at the same temperature, T. The α value is calculated as the ratio of partial area of the crystallization peak at T to the total area of the crystallization that is exothermic. The activation energies values are $E_{T_g} = 648$ kJ/mol for V1 and 685 kJ/mol for V3, while $E_{cr} = 454$ kJ/mol for V1 and 334 kJ/mol for V3. The reaction order was evaluated as 2.3 for V1 (at 870 °C) and as 1.5 for V3 (at 950 °C). These values confirm the tendency for bulk crystallization in V1 and of surface crystallization in V3 [9,14]. The bulk phase formation in V1 and the surface crystallization in V3 were confirmed also by SEM observation. Fig. 4(a) shows the interior part of a V1 sample with bulk spherulitic and dendritic structures, formed after 2 h at 900 °C (i.e. the temperature of the DTA peak onset). V3 glass-ceramic shows elongated crystals. The selected heat treatment is typical for similar compositions

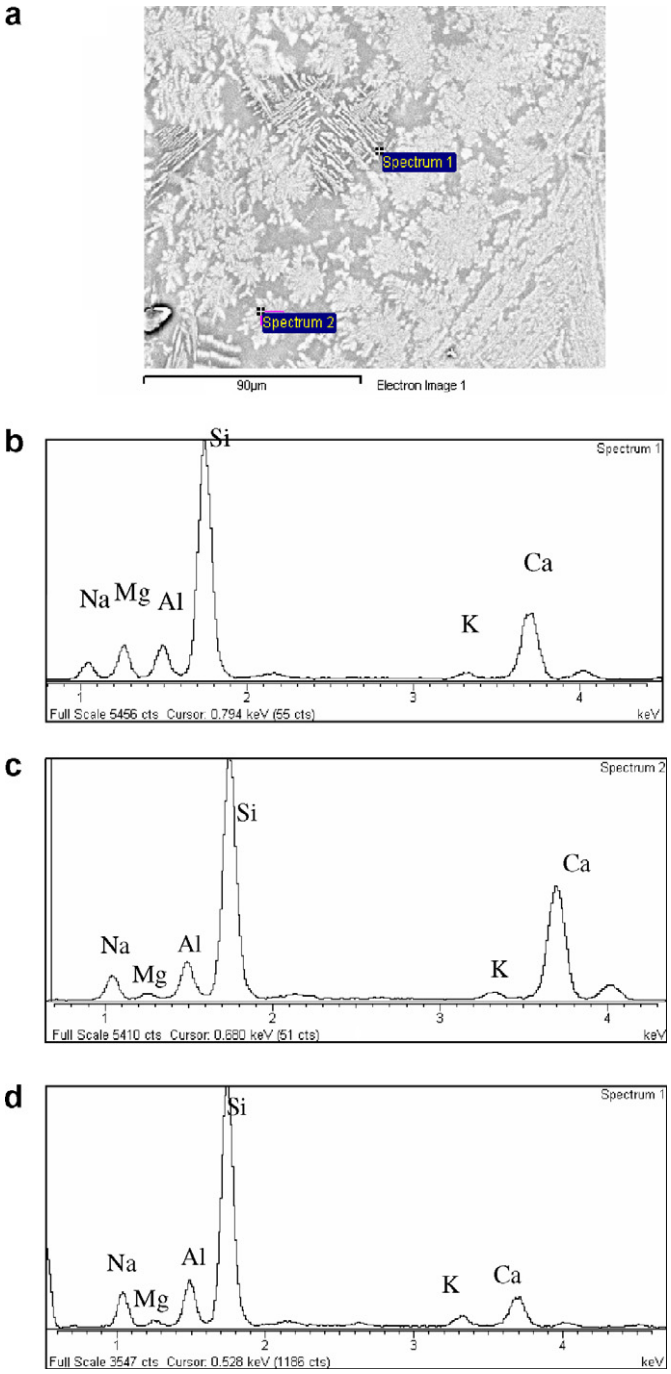

Fig. 4. (a) SEM micrograph of V1 glass-ceramic treated at 900°C for 2 h, (b) and (c) EDS spectra of different crystals, (d) EDS spectrum of the glassy matrix.

and corresponds to the temperature range of maximum rate of crystal growth [19–21]. The crystalline phase formation starts from the surface with needle-like crystals oriented towards the interior of the sample.

The crystalline phases developed in V1 and V3 glass-ceramics have been identified by X-ray diffraction. The only phase identified in V3 is wollastonite ($CaSiO_3$), whereas the number and kind of crystalline phases formed in V1 depends on the applied thermal treatment. The first phases formed in V1 are calcium silicates $CaSiO_3$ (triclinic pseudowollastonite as main phase, and monoclinic wollastonite as minor phase), already at low temperature (900 °C) and short times (30 min) (Fig. 5). For longer firing times, however, an increase of the amount of monoclinic wollastonite is detected. These phases commonly occur in cements, ceramics, and glass-ceramic materials produced starting from slags [9,10,22,23]. For longer times, it was found that pyroxene solid solutions also crystallized. As shown in Fig. 5, peaks of the pyroxene phase appear only for the samples heat-treated for 2 h.

SEM images of V1 glass-ceramics (Fig. 4) show two kinds of crystals: the main with spherulitic shape enriched in calcium and devoid of magnesium, which corresponds to pseudowollastonite and/or wollastonite. The weight percentage of Ca and Mg, analyzed by EDS, are 16% and 0.7%, respectively in the glass-ceramics (Fig. 4(c)), while they are 3.3% and 0.65% in the residual glass (Fig. 4(d)). Residual glass shows a strong decrease of calcium with respect to the starting glass (CaO > 20%, MgO > 2.5%), because of the formation of calcium based crystalline phases. The secondary phase, formed in the residual glass matrix with dendritic structure shows pyroxene composition enriched in magnesium (4%) (Fig. 4(b)). In V3 glass-ceramic elongated crystals rich in Si and Ca are present, which correspond to wollastonite, and the residual glass shows a corresponding decrease of calcium content with respect to the starting glass.

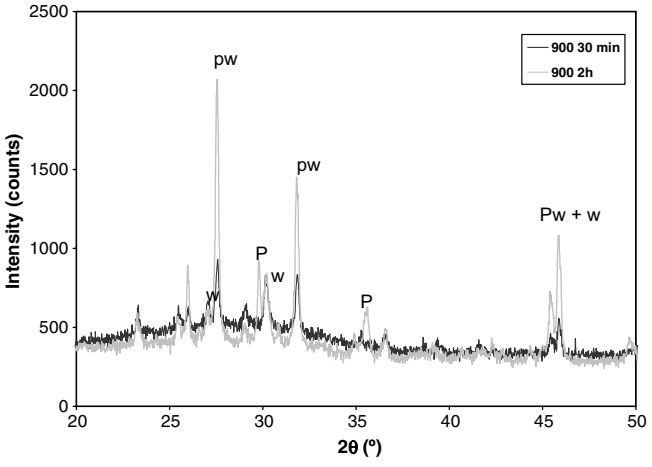

Fig. 5. XRD patterns of V1 glass-ceramics treated at 900 °C for 30 min (black line) and 2 h (gray line).

4. Discussion

4.1. Structure and chemical durability

The difference in the homogeneity of V1 and V2 glasses may be related to the substitution of the easily meltable glass cullet (which favors the atoms mobility in the melt and the homogenization process) with the feldspar waste, which increases the viscosity during the melting.

The phase separation phenomenon, with a non-spinodal structure, present in V1 and the immiscibility zones present in V2 may be ascribed to by the 'reduced composition' of the glasses. These reduced compositions are V1: 67.9% SiO_2–6.8%Al_2O_3–25.3%CaO; V2: 64.1%SiO_2–14.8% Al_2O_3–21.1%CaO. Fig. 6 shows that a liquid immiscibility area exists near the CaO–SiO_2binary system. In the ternary diagram (Fig. 6(a)) V1 is situated nearer to the phase separation area with respect to V2, confirming the larger amount of immiscibility drops emerged by SEM analysis for the sample V1 (Fig. 1(a)). On the other hand, V2 is located nearer to the tridymite–pseudowollastonite–anorthite eutectic point; therefore it shows less phase separation. The inhomogeneous zones of V2, present in Fig. 1(b), can be a silica-enriched phase because during melting, the quartz particles, which are the main crystalline phase in the bottom ash, cannot completely melt because of

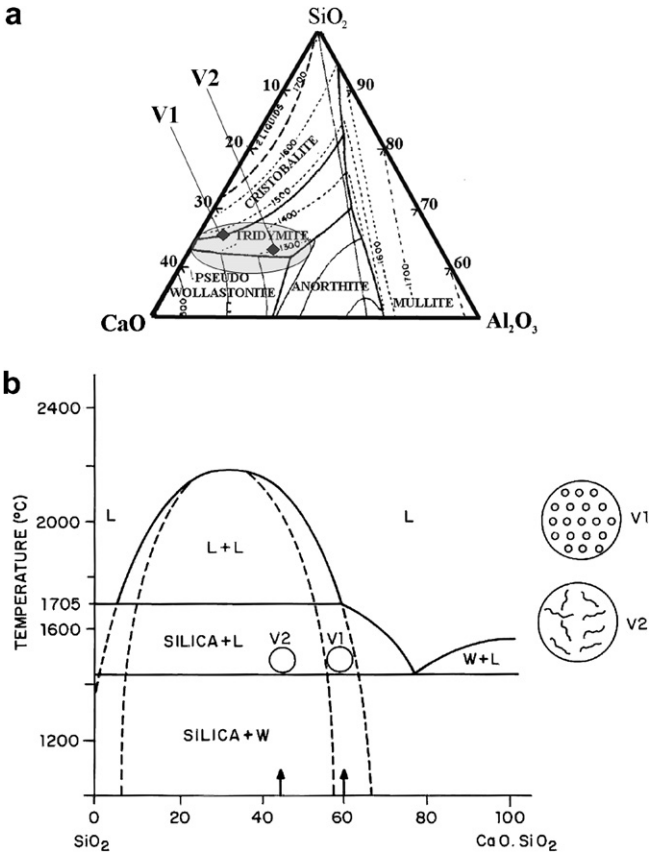

Fig. 6. (a) ternary diagram SiO_2–CaO–Al_2O_3 and (b) binary immiscibility curve.

the high viscosity. According to the $CaO–SiO_2$ liquid immiscibility curve (Fig. 6(b)) and on reducing the ternary composition to this binary, V2 glass is located in the spinodal region of immiscibility. Therefore the pseudo-dendritic texture of V2 seen in Fig. 1(b) may be explained by spinodal immiscibility areas produced by diffusion around some silica particles (indicating lower degree of homogenization). V1 is characterized with good transparency and dark-green color; in this case the glass is located in the nucleation area for phase separation, giving rise to smaller sized droplets (Fig. 1(a)).

The difference in the chemical durability behavior of both glasses is due to the higher amount of alumina in V2, which strengthens the glassy network playing the role of network former, and to the higher amount of alkaline mobile ions, especially Na^+ in V1. This behavior is also confirmed by pH and conductivity measurements. In fact, the values of these properties increase because of both the release in solution of monovalent alkaline oxides and because of the ionic exchange between H^+ ions of water and alkaline ions of glass. These ions are the most mobile ions in the glass lattice, because they are placed within the interstices and are linked with low bond strength (non-bridging oxygen).

The more significant difference between the behavior of V1 and V2 in the aqueous environment with respect to the alkaline one is related to the different attack mechanism. In fact, in water both H^+ and OH^- ions occur, while in alkaline environment OH^- ions are predominant. Since the H^+ attack is strictly related to the ionic exchange with alkaline ions, therefore is more significant in V1 glass where the amount of Na^+ and K^+ is higher than in V2. At the same time, the OH^- interaction is similar in both glasses because it acts directly on the glassy network, which is constituted mainly of silicon and aluminum tetrahedral.

4.2. Crystallization behavior

The thermal study performed shows both the different tendency toward crystallization of the three glasses, evidenced by Hruby coefficient, and the different crystallization mechanism. In fact the reaction order values, determined by Ozawa equation, suggest that bulk crystallization occurs in V1, and surface crystallization occurs in V3 [9,14]. The two glasses have similar E_{T_g} values while E_{cr} of V1 is notably higher than E_{cr} of V3. At the same time, both E_{T_g} and E_{cr} values of V1 and V3 are in good agreement with the hypothetical activation energies of viscous flow for the corresponding temperature ranges (Table 3). This indicates that diffusion-controlled crystal growth occurs in both compositions [14] and demonstrates that the higher E_{cr} value of V1 is due to its superior crystallization tendency, which leads to a phase formation at lower temperature and higher viscosity.

As regards the crystalline phases formed in the heat-treated glasses, pseudowollastonite is the main phase in all samples, notwithstanding the fact that it is the high temperature $CaSiO_3$ form; in fact at temperatures lower than 1125 °C, the stable phase is the monoclinic wollastonite modification [24]. The stability of pseudowollastonite at low temperature can be explained considering the presence in the glasses of copper sulfide, formed by the oxidation of copper metal in the presence of sulfur, due to the incinerator residues composition (see Fig. 1). According to Kaitai et al. who found ZnS to be a nucleating agent for the formation of pseudowollastonite before wollastonite [25], CuS can modify the equilibrium of these two polymorphs phases. The pseudowollastonite transforms to wollastonite or diopside when heat treatment temperature or time is higher. The formation of pyroxene solid solution requires longer thermal treatments because of the high amount of CaO in V1 (>20 wt%): firstly the calcium silicates precipitate and then, when the residual glass composition is depleted of calcium and the Ca/(Mg + Fe) ratio decreases, the pyroxenes formation begins.

5. Conclusions

From the conducted study it appears that the vitrification process applied to the tailored mixtures is a useful technique to immobilize the incinerator wastes in chemically stable matrices. The obtained glasses are technologically interesting because they show good chemical resistance, in particular in alkaline environment. This is an important characteristic, especially for the V2 glass, which due to its scarce crystallization tendency, is suitable for manufacturing glass products such as fibers and/or tiles [6,7]. From the thermal characterization it appears that the materials are also suitable to obtain glass-ceramic. It was concluded that V1 glass is more appropriate for the obtainment of glass-ceramics by bulk nucleation and growth, while V3, presenting a reduced crystallization, is more adequate for manufacturing sintered glass-ceramic material, where the surface nucleation mechanism is exploited [9,14,19,20].

Acknowledgments

Authors would like to thank MIUR of Italy (Project PRIN 2003 ‘Materiali polifasici a matrice vetrosa ed ecocompatibili da recupero di residui inorganici a base di ossidi provenienti da attività industriali: progettazione e modellazione’) and PRRIITT Regional Project (LITCAR ‘Laboratorio Integrato Tecnologie e Controllo Ambientale nel Ciclo di vita dei Rifiuti’) for the financial support.

References

[1] J.M. Chimenos, M. Segarra, M.A. Fernandez, F. Espiell, J. Hazard. Mater. 64 (1999) 211.
[2] M. Ferraris, M. Salvo, F. Smeacetto, L. Augier, L. Barbieri, A. Corradi, I. Lancellotti, J. Eur. Ceram. Soc. 21 (4) (2001) 453.
[3] S. Abe, F. Kambayashi, M. Okada, Waste Manage. 16 (1996) 431.
[4] A.R. Boccaccini, H. Kern, in: Proceedings of the R’99 World Congress on Recovery Recycling Re-integration, vol. II, Geneva, Switzerland, 1999, EMPA, St. Gallen, Switzerland, 1999, p. 152.

[5] M. Nishigaki, Waste Manage. 20 (2000) 185.
[6] P. Colombo, G. Brusatin, E. Bernardo, Scarinci, et al., Curr. Opin. Solid State Mater. Sci. 7 (3) (2003) 225.
[7] R.D. Rawlings, J. Wu, A.R. Boccaccini, J. Mater. Sci. 41 (3) (2006) 733.
[8] J. Rincon, A. Duran, Separación de Fases en Vidrios, Ed. Soc. Esp. Ceram. Vidr., 1982, Arganda del Rey, Madrid, p. 127.
[9] Z. Strnad, Glass–Ceramic Materials, Elsevier, Amsterdam, 1986.
[10] V.V. Polak, P.D. Sarkisov, V.F. Solinov, M.A. Carazin, Technology of building glass and slag-sitalls, in Russian, Sroiisdat, Moscow, 1983.
[11] M. Aloisi, A. Karamanov, L. Arrizza, F. Ferrante, I. Matekovits, M. Ferraris, M. Pelino, in: Proceedings of the 5th International Congress 'Added Value and Recycling of Industrial Wastes' VARIREI 2005, L'Aquila (Italy), 26–30, 06, 2005 (CD).
[12] J.E. Shelby, W.C. Lacourse, A.G. Clare, Engineering properties of oxide glasses and other inorganic glasses, in: S.J. Schneider (Ed.), Engineered Materials Handbook, vol. 4, ASM, 1991, p. 845.
[13] H. Sholze, Glass Nature, Structure and Properties, Springer Verlag, Berlin, New York, 1990.
[14] W. Hołand, G. Beall, Glass-ceramics Technology, The American Ceramics Society, Westerville.
[15] J. Sestak, Thermophysical Properties of Solids – Their Measurements and Theoretical Thermal Analysis, Academia Prague, 1984.
[16] I. Avramov 1, E.D. Zanotto, M.O. Prado, J. Non-Cryst. Solids 320 (2003) 9.
[17] H. Chen, J. Non-Cryst. Solids 27 (1978) 257.
[18] T. Ozawa, Polymer 12 (1971) 150.
[19] A. Karamanov, I. Gutzow, I. Penkov, Glastech. Ber., Glass Sci. Technol. 67 (7) (1994) 202.
[20] A. Karamanov, M. Pelino, M. Ferraris, I. Matecovitz, J. Eur. Ceram. Soc. 23 (2003) 1609.
[21] V.M. Fokin, M.L.F. Nascimento, E.D. Zanotto, J. Non-Cryst. Solids 351 (10–11) (2005) 789.
[22] H. Yang, C.T. Prewitt, Am. Mineral. 84 (1999) 929.
[23] T. Toya, Y. Kameshima, A. Yasumori, K. Okada, J Eur. Ceram. Soc 24 (2004) 2367.
[24] W. Deer, R. Howie, J. Zussman, An Introduction to the Rock-forming Minerals, 2nd Ed., Longman Scientific & Technical, 1992.
[25] W. Kaitai, L. Hanliang, C. Youxin, S. Dingkun, Chin. Acad. Sci. 11 (2) (1996) 214.